



# HHS Public Access

Author manuscript

*Leukemia*. Author manuscript; available in PMC 2016 August 22.

Published in final edited form as:

*Leukemia*. 2016 June ; 30(6): 1355–1364. doi:10.1038/leu.2016.35.

## High affinity FR $\beta$ -specific CAR T cells eradicate AML and normal myeloid lineage without HSC toxicity

Rachel C Lynn<sup>1</sup>, Yang Feng<sup>2</sup>, Keith Schutsky<sup>1</sup>, Mathilde Poussin<sup>1</sup>, Anna Kalota<sup>3</sup>, Dimiter S Dimitrov<sup>2</sup>, and Daniel J Powell Jr<sup>1,4</sup>

<sup>1</sup>Ovarian Cancer Research Center, Department of Obstetrics and Gynecology, Perelman School of Medicine, University of Pennsylvania, Philadelphia, PA 19104, USA

<sup>2</sup>Protein Interactions Section, Cancer and Inflammation Program, Center for Cancer Research, National Cancer Institute, Frederick, MD 21702, USA

<sup>3</sup>Division of Hematology and Oncology, Abramson Cancer Center, University of Pennsylvania, Philadelphia, PA 19104, USA

<sup>4</sup>Department of Pathology and Laboratory Medicine, Abramson Cancer Center, Perelman School of Medicine, University of Pennsylvania, Philadelphia, PA 19104, USA

### Abstract

Acute myeloid leukemia (AML) is an aggressive malignancy, and development of new treatments to prolong remissions is warranted. Chimeric antigen receptor (CAR) T-cell therapies appear promising but on-target, off-tumor recognition of antigen in healthy tissues remains a concern. Here, we isolated a high affinity (HA) folate receptor beta (FR $\beta$ )-specific scFv (2.48nM K<sub>D</sub>) for optimization of FR $\beta$ -redirected CAR T-cell therapy for AML. T-cells stably expressing the HA-FR $\beta$  CAR exhibited greatly enhanced antitumor activity against FR $\beta$ <sup>+</sup> AML *in vitro* and *in vivo* compared to a low affinity (LA) FR $\beta$  CAR (54.3nM K<sub>D</sub>). Using the HA-FR $\beta$  IgG, FR $\beta$  expression was detectable in myeloid-lineage hematopoietic cells; however, expression in CD34<sup>+</sup> hematopoietic stem cells (HSCs) was nearly undetectable. Accordingly, HA-FR $\beta$  CAR T-cells lysed mature CD14<sup>+</sup> monocytes, while HSC colony formation was unaffected. Because of the potential for elimination of mature myeloid lineage, mRNA CAR electroporation for transient CAR expression was evaluated. mRNA-electroporated HA-FR $\beta$  CAR T-cells retained effective anti-tumor activity *in vitro* and *in vivo*. Together, our results highlight the importance of antibody affinity in target protein detection and CAR development and suggest that transient delivery of potent HA-FR $\beta$  CAR T-cells is highly effective against AML and reduces the risk for long-term myeloid toxicity.

Users may view, print, copy, and download text and data-mine the content in such documents, for the purposes of academic research, subject always to the full Conditions of use:[http://www.nature.com/authors/editorial\\_policies/license.html#terms](http://www.nature.com/authors/editorial_policies/license.html#terms)

**Corresponding Author:** Daniel J. Powell Jr., Ph.D., University of Pennsylvania, 3400 Civic Center Blvd, Bldg. 421, Smilow CTR, Rm 08-103, Philadelphia, PA 19104-5156, Phone: 215-573-4783, Fax: 215-573-7627, [poda@mail.med.upenn.edu](mailto:poda@mail.med.upenn.edu).

#### Conflicts of Interest

The authors have no conflicts of interest to disclose related to the work described.

#### Authorship

RCL and DJP designed experiments and wrote the paper. RCL conducted experiments, analyzed data and prepared the figures. YF and DSD isolated the scFvs and prepared and conducted experiments with soluble FR $\beta$  scFvs and IgGs. KS prepared mRNA CAR reagents. MP conducted *in vivo* imaging. AK scored the CFU. All authors have read and approved the submitted manuscript.

## Introduction

Acute myeloid leukemia (AML) remains a disease with poor prognosis<sup>1, 2</sup>. Currently, the most effective therapy, allogeneic bone marrow transplant, is not feasible in all patients, may not fully eliminate tumor cells, and carries a substantial risk of GVHD-associated toxicity<sup>3-5</sup>. Therefore, newer safe and effective therapy is needed for AML. Chimeric antigen receptor (CAR) T-cell therapy has recently produced dramatic clinical success in patients with CD19<sup>+</sup> acute and chronic lymphocytic leukemia with up to 90% of patients responding<sup>6-8</sup>. CAR T-cells are genetically modified to eliminate tumor cells by linking extracellular tumor antigen-recognition domains, most commonly antibody-derived single-chain variable fragments (scFvs), to intracellular T-cell receptor signaling moieties<sup>9</sup>. Expanding the clinical efficacy of CD19-directed CAR therapy to additional types of cancer will depend foremost on the identification of appropriate cell-surface tumor antigens. In the application of cytolytic CAR T-cells, the largest concern remains toxicity resulting from off-tumor CAR recognition of target protein in healthy tissues.

The high expression of several AML surface antigens, such as CD33 and CD123, on healthy bone marrow (BM) hematopoietic stem cells (HSCs) remains a prominent challenge for developing safe and effective CAR therapy for AML<sup>10-14</sup>. We have previously established that folate receptor beta (FR $\beta$ )-specific CAR T-cells can target AML without HSC toxicity<sup>15</sup>. However, these CAR T-cells were functionally limited, effectively controlling AML tumor growth only in the minimal disease setting. Modifying CAR platforms with high affinity scFvs can result in improved anti-tumor activity<sup>16, 17</sup>. However, higher affinity CARs may possess heightened sensitivity to antigen on healthy tissues and present a greater risk for off-tumor toxicity in patients. Indeed, toxicity related to off-tumor recognition has led to patient morbidity in clinical trials using CAR T-cells redirected against Her2<sup>18</sup> and CAIX<sup>19</sup>.

Awareness of target tumor antigen expression in normal tissues is exceedingly important for the prediction of possible off-tumor toxicity. Because the antigens targeted in CAR T-cell therapy are commonly self-antigens, with overexpression on tumor cells, it is not uncommon for low levels of antigen to be expressed on normal tissues<sup>20</sup>. Antibodies are commonly used to assess protein expression by tumor and healthy cells using flow cytometry or IHC, however antibody affinity should be carefully considered as lower affinity reagents may be unable to bind low levels of antigen and therefore produce false-negative results.

We hypothesized that our previously described FR $\beta$ -specific scFv, which bears low-intermediate affinity (LA) for FR $\beta$ , may not promote optimal interaction with FR $\beta$ , either in a CAR platform or as a labeling reagent. Therefore, we sought to develop high affinity (HA) reagents for FR $\beta$  CAR platform optimization as well as sensitive protein detection in normal tissues to better assess potential risk for toxicity related to targeting FR $\beta$  in AML.

## Materials and Methods

### Surface plasmon resonance analysis

Binding of LA-FR $\beta$  or HA-FR $\beta$  Fab to recombinant human FR $\beta$  (rFR $\beta$ ) was assessed using Biacore $\times$ 100 instrument as described<sup>21</sup>. Briefly, purified rFR $\beta$  was immobilized on a CM5 sensor chip. LA-FR $\beta$  or HA-FR $\beta$  scFv, diluted to 0.04, 0.4, 4, 40, or 400 nM, was applied through the cells. The chip was regenerated with 10 mM glycine pH 2.5, 1 M NaCl. The sensorgram was analyzed with BiaEvaluation software, and data were fitted to a 1:1 binding model.

### rFR $\beta$ binding ELISA

100 ng/well rFR $\beta$  was coated on 96-well plates overnight at 4°C. Wells were blocked and 50 $\mu$ L of diluted antibodies were incubated 2h at 37°C in duplicate. 1:1000 goat anti-human IgG-HRP (Jackson ImmunoResearch) for 1h at 37°C and 50 $\mu$ L/well ABTS substrate were used for detection of LA-FR $\beta$  and HA-FR $\beta$  IgG binding. Absorbance was read at 405 nm.

### Lentiviral CAR Production

The HA-FR $\beta$  scFv was cloned into previously validated pELNS lentiviral vectors containing CD3 $\zeta$  or CD28-CD3 $\zeta$  to create HA-Z and HA-28Z CAR constructs (details and sequences in supplement). Third generation lentiviral vector was produced in 293T (ATCC) as previously described<sup>15, 22</sup>. Briefly, 293Ts were transfected with pRSV-Rev, pMDLg/pRRE, pMD2.G and pELNS CAR plasmids. 24h and 48h supernatants were combined and concentrated using high-speed ultracentrifugation. Lentiviral vectors were titered in 293Ts and stored at -80°C until use.

### Cells

All cells were cultured in complete media (CM, RPMI-1640-GlutaMAX, 10% FBS, 100U/mL penicillin, 100 $\mu$ g/mL streptomycin) at 37°C. C30<sup>23</sup> was provided by George Coukos. C30-FR $\beta$  was created as described<sup>15</sup>. Human AML cell lines THP1, MV411, and HL60 were provided by Gwenn Danet-Desnoyers. Cell lines used in animal models were confirmed mycoplasma negative before use. De-identified healthy adult BM, CD34<sup>+</sup> HSCs and primary human AML were purchased from the University of Pennsylvania Stem Cell and Xenograft Core (SCXC). Peripheral blood (PB) was collected by apheresis from volunteer donors by the University of Pennsylvania Human Immunology Core (HIC) with informed consent according to the Declaration of Helsinki. Whole blood, monocytes, and T-cells were purchased from HIC. T-cells were activated, transduced, and expanded as previously described<sup>15, 22</sup>. Briefly, T-cells were activated with  $\alpha$ CD3/ $\alpha$ CD28 beads, lentivirally transduced at MOI=10 20h later, and expanded in CM with 50IU/mL IL2 for 10–14 days. Cell size was monitored using a Multisizer-3 Coulter Counter (Beckman Coulter). Rested T-cells (<300fL volume) were used for functional *in vitro* and *in vivo* assays. Transduction frequencies were normalized using untransduced T-cells before each experiment.

## Flow Cytometry

Up to  $1 \times 10^6$  cells were labeled in 100 $\mu$ L staining buffer (2% FBS in PBS) containing relevant antibodies for 30min at 4°C. LA-FR $\beta$  and HA-FR $\beta$  scFv and IgG were prepared as described and biotinylated *in vitro*. 0.5 $\mu$ g IgG or 1 $\mu$ g scFv was used for primary labeling, and 1:200 Streptavidin (SA)-APC for secondary detection. Washed samples were assessed by flow cytometry using a FACSCantoII flow cytometer (BD) in the presence of 7AAD. Surface CAR was labeled using 0.3 $\mu$ g rabbit-anti-human-IgG(H+L)-biotin (LA-FR $\beta$ , HA-FR $\beta$ , or CL10 CARs) or 0.3 $\mu$ g goat-anti-mouse-IgG(H+L)-biotin (CD19 CAR) and secondary SA-APC or PE. Marker antibody details in supplement.

## CAR binding to rFR $\beta$

GFP-2A-CAR constructs were used to evaluate binding to rFR $\beta$  by flow cytometry. rFR $\beta$  was biotinylated *in vitro*.  $2 \times 10^5$  T-cells were incubated with 200ng, 500ng, or 1 $\mu$ g rFR $\beta$ -biotin and secondary SA-APC. For CAR T-cell reactivity against rFR $\beta$ , 250 or 500ng rFR $\beta$  was coated on 96-well plates overnight at 4°C. Wells were washed and  $1 \times 10^5$  CAR $^+$  T-cells/well were cultured overnight in 200 $\mu$ L CM. IFN $\gamma$  secretion was assessed by ELISA.

## Cytokine Release and CD69

$1 \times 10^5$  targets and  $1 \times 10^5$  CAR $^+$  T-cells were plated in 200 $\mu$ L CM. After overnight co-culture, supernatants were analyzed by IFN $\gamma$  ELISA. IFN $\gamma$ , IL2, MIP1 $\alpha$ , TNF $\alpha$ , IL4, and IL10 were assessed using cytokine bead array (BD). In some cases, cell pellets were washed and labeled for CD3, CAR, and CD69 by flow cytometry following co-culture.

## Cell Lysis

Cell lines C30, C30-FR $\beta$ , THP1, MV411, and HL60 were stably transduced with GFP-2A-firefly luciferase (fLuc) lentiviral vector.  $2 \times 10^4$  fLuc-targets were cultured in white 96-well plates with CAR $^+$  T-cells at 5:1, 1:1, and 1:5 E:T ratios in triplicate. After overnight co-culture, residual luciferase activity was measured using the Extended-Glow Luciferase Reporter Gene Assay System (Life Technologies). Percent lysis was calculated as follows [100– ((Average Signal T-cell Treated Wells)/(Average Signal Untreated Target Wells)  $\times$  100)].

## Degranulation

$1 \times 10^5$  target cells and  $1 \times 10^5$  CAR $^+$  T-cells were plated in 200 $\mu$ L CM with monensin and 5 $\mu$ L/well CD107a-APC and CD107b-APC in triplicate. After 6h co-culture, total cells were labeled for CD3, CAR and 7AAD by flow cytometry.

## CFU Assay

2000 healthy adult BM CD34 $^+$  HSCs were cultured with 2000 CAR $^+$  T-cells in V-bottom plates. After 4h, wells were diluted in methylcellulose and plated in duplicate. After 14 days colonies were counted and scored as CFU-GEMM, GM, G, M, or BFU-E.

### BM Lysis Assay

$1 \times 10^5$  CD34<sup>(-)</sup> BM cells and  $1 \times 10^5$  CAR<sup>+</sup> T-cells were plated in 200 $\mu$ L CM. After 5h, cells were washed and labeled for CD3, CD33, CD19, FR $\beta$  and 7AAD. The phenotype of cells surviving co-culture is indicated in represented flow cytometry plots.

### Monocyte Lysis

$2 \times 10^4$  healthy donor monocytes were labeled with Cr<sup>51</sup>, washed, and plated with CAR<sup>+</sup> T-cells at the indicated E:T ratios in 6 replicates. Monocyte lysis was assessed after 4h by Cr<sup>51</sup> release. Spontaneous release was measured in untreated target wells. Maximum lysis was induced with 10% SDS. Percent Lysis = [(Treated–Spontaneous)/(Maximum–Spontaneous)  $\times$  100].

### Mice

6–8 week old male or female Nod/SCID/ $\gamma$ chain<sup>-/-</sup> (NSG) and Nod/SCID/ $\gamma$ chain<sup>-/-</sup> with transgenic human SF, GM-CSF, and IL3 (NSGs) mice were purchased from, treated and maintained under pathogen-free conditions by the SCXC under protocols approved by the University of Pennsylvania IACUC. We injected  $5 \times 10^6$  fLuc-THP1 tumor cells subcutaneously (sc) or intravenously (IV) and T-cells intraperitoneally (IP) or IV as indicated in the figure legends. Tumor growth was monitored by caliper measurement (sc models) and bioluminescent imaging as described<sup>15</sup>. Mice were randomized to ensure equal mean tumor burden between groups before treatment. 5 mice per group were treated based on previous tumor models<sup>15</sup>. Researchers were blinded to treatment groups during data acquisition. Peak luminescence is displayed as p/s (IV tumor) or p/s/cm<sup>2</sup> (sc tumor). Peripheral blood sampling was conducted via retro-orbital blood collection under isoflurane anesthesia. 50 $\mu$ L blood was labeled for indicated cell markers and quantified using TRUCount beads (BD).

### mRNA CAR

pELNS lentiviral CAR constructs were digested and ligated into PDA mRNA expression plasmids. mRNA was produced *in vitro* as described<sup>24</sup>. T-cells were electroporated with 10 $\mu$ g mRNA/ $10 \times 10^6$  cells using an ECM830 BTX electroporator (Harvard Apparatus) at the following settings: unipulse, 500V, 700 $\mu$ s. “No-RNA” T-cells were electroporated without mRNA. mRNA-CAR expression and functional activity were assessed at the indicated time points following electroporation.

### Statistical Analysis

Data was analyzed for significance using an unpaired two-tailed student’s t-test using the Holm-Sidak method without assuming a consistent SD (GraphPad Prism 6). P < .05 was considered significant. All error bars represent mean and standard error (SEM) unless otherwise noted in figure legends. Specific sample sizes and experimental replicates are reported in the figure legends. Unless otherwise noted, *in vitro* assays were repeated at least 3 times to ensure adequate power.

## Results

### Isolation of a higher affinity FR $\beta$ scFv

To identify high affinity FR $\beta$ -specific antibodies, we isolated a new scFv through light chain shuffling as previously described<sup>25</sup>. We utilized Biacore  $\times 100$  (Figure 1a) to define monovalent affinities of 54.3nM for LA-FR $\beta$ <sup>15</sup> and 2.48nM for the new high affinity (HA) FR $\beta$  scFv. HA-FR $\beta$  IgG displayed increased binding capability to rFR $\beta$  protein by ELISA (Figure 1b) and cell-surface FR $\beta$  by flow cytometry (Figure 1c). FR $\beta$ <sup>+</sup> cell lines C30-FR $\beta$ , THP1 and MV411 all displayed greater binding to HA-FR $\beta$  IgG as visualized by increased MFI compared to LA-FR $\beta$  IgG. The HA-FR $\beta$  scFv was also able to bind THP1 and MV411, albeit at lower levels compared to the full bivalent IgG, whereas the LA-FR $\beta$  scFv could not be visualized by flow cytometry (Figure S2). Although the epitopes recognized by LA-FR $\beta$  and HA-FR $\beta$  scFvs have not been defined, competition ELISAs demonstrate their ability to inhibit association of the other to rFR $\beta$  (Figure S3), suggesting binding at nearby locations.

### High affinity FR $\beta$ CAR T-cells demonstrate increased binding to rFR $\beta$

The HA-FR $\beta$  scFv was cloned into previously validated lentiviral CAR vectors containing either CD3 $\zeta$  alone or CD28-CD3 $\zeta$  intracellular signaling domains to create HA-Z and HA-28Z CAR constructs, respectively (Figure 1d and S4a). Primary human T-cells were transduced with lentiviral CAR constructs, and transduction efficiency was determined by labeling for surface CAR expression. Control T-cells were transduced with GFP, CD19-28Z CAR, or CL10-28Z CAR (specific for mouse FR $\beta$ ). High transduction efficiencies were reproducibly achieved (Figure S4b). GFP-2A-LA-FR $\beta$  and HA-FR $\beta$  CAR T-cells were labeled with rFR $\beta$ , and binding of cell-surface CAR to recombinant antigen was determined by flow cytometry. HA-FR $\beta$  CAR T-cells demonstrated high association with rFR $\beta$ , whereas this interaction could barely be visualized with LA-FR $\beta$  CAR even at high protein concentration (Figure 1e). Accordingly, HA-FR $\beta$  CAR T-cells also exhibited increased IFN $\gamma$  production in response to immobilized rFR $\beta$  *in vitro* (Figure 1f).

### High affinity FR $\beta$ CAR T-cells display increased reactivity against cell surface FR $\beta$

Next we assessed the relative functional reactivity of low and high affinity CAR T-cells against cell surface FR $\beta$  by measuring T-cell cytokine secretion, CD69 expression, and lytic activity against FR $\beta$ <sup>+</sup> cell lines C30-FR $\beta$ , THP1 and MV411 and FR $\beta$ <sup>(-)</sup> cell lines C30 and HL60. Compared to LA-FR $\beta$ , HA-FR $\beta$  CAR T-cells secreted dramatically increased levels of IFN $\gamma$  in the presence of FR $\beta$ <sup>+</sup> C30-FR $\beta$ , THP1 and MV411 without activity against negative lines (Figure 2a). HA-FR $\beta$  CAR T-cells also produced high levels of IL2 and MIP1 $\alpha$ , and moderate to low levels of TNF $\alpha$ , IL4, and IL10 (Figure S5). As depicted in Figure 2b, >90% of LA-FR $\beta$  and HA-FR $\beta$  CAR<sup>+</sup> T-cells upregulated CD69 in the presence of high density FR $\beta$  (C30-FR $\beta$ ). However, when encountering antigen at endogenous levels on the AML cell lines, LA-FR $\beta$  CAR T-cells displayed lower levels of CD69, whereas nearly all HA-FR $\beta$  CAR T-cells were positive. Likewise, both LA-FR $\beta$  and HA-FR $\beta$  CARs displayed high lytic activity against C30-FR $\beta$  (Figure 2c); however, only HA-FR $\beta$  T-cells efficiently lysed THP1 and MV411 AML with endogenous FR $\beta$  expression.

To determine whether soluble FR $\beta$  IgGs could block CAR T-cell activity, we measured IFN $\gamma$  secretion in response to C30-FR $\beta$  in the presence of LA-FR $\beta$  or HA-FR $\beta$  blocking IgGs. High concentrations (>40ng/1 $\times$ 10<sup>5</sup> target cells) of HA-FR $\beta$  IgG completely blocked LA-FR $\beta$  CAR T-cell IFN $\gamma$  secretion (Figure S6). Interestingly, neither low nor high affinity IgG was able to block activity of HA-FR $\beta$  CAR T-cells.

### High affinity FR $\beta$ CAR T cells display exceptional anti-leukemic activity *in vivo*

To determine whether the potent activity of HA-FR $\beta$  CAR T-cells against AML could be recapitulated in a mouse model of human disease, we inoculated immunocompromised NSG mice with FR $\beta$ <sup>+</sup> fLuc-THP1 human AML. Previously, in mice treated with T-cells at days 8 and 10 of tumor growth, both LA-FR $\beta$  and HA-FR $\beta$  CAR T-cells led to long-term tumor control<sup>15</sup> (and data not shown). Here, we evaluated FR $\beta$  CAR T-cells in mice with large, palpable subcutaneous AML tumors. Surprisingly, both first and second generation HA-FR $\beta$  CAR T-cells reproducibly mediated rapid and enduring complete tumor destruction (Figure 3a). LA-FR $\beta$  CAR T-cells were ineffective. Consistent with robust *in vivo* activation, peripheral HA-FR $\beta$  CAR T-cell numbers were significantly elevated 2 weeks post treatment whereas LA-28Z CAR T-cell counts were not different from control T-cell treated mice (day 29; Figure 3b). However, at day 42, LA-28Z CAR T-cells were present at very high frequency (Figure 3b) while HA-FR $\beta$  CAR T-cell numbers from mice that had cleared tumor were low but detectable. Thus, chronic activation of LA-FR $\beta$  CAR T-cells in the continued presence of FR $\beta$ <sup>+</sup> tumor *in vivo* led to robust expansion, however, likely due to their low functional avidity, did not result in efficient activity against large tumor burden. Alternatively, HA-FR $\beta$  CAR T-cells were efficiently activated by FR $\beta$ <sup>+</sup> AML, transiently expanded *in vivo*, rapidly cleared tumor and numerically contracted, illustrating an antigen-dependent mechanism of CAR T-cell persistence *in vivo*.

Despite their numerical contraction following clearance of tumor, HA-Z and HA-28Z CAR T-cells were still detectable at on day 92 (Figure S7), suggesting the potential for long-lasting tumor protection. To directly assess this hypothesis, we re-challenged mice that had previously eradicated their primary tumor (HA-28Z) or that were previously untreated (naïve) with 5 $\times$ 10<sup>6</sup> THP1 cells on the opposite flank. Previous treatment led to complete protection against tumor re-challenge (Figure 3c).

### High affinity FR $\beta$ CAR T-cells are reactive against primary human AML

Importantly, HA-FR $\beta$  CAR T-cells also recognized primary human AML. Previous reports found that 70% of AML patients express FR $\beta$ <sup>26, 27</sup>. Using HA-FR $\beta$  IgG, we confirmed expression of FR $\beta$  in 15/16 (93.8%) of AML specimens by flow cytometry, with a mean of 49.8% FR $\beta$ <sup>+</sup> blasts (Figure 4a). Four samples with varying FR $\beta$  expression were used to assess CAR function. Both LA-FR $\beta$  and HA-FR $\beta$  CAR T-cells secreted significantly more IFN $\gamma$  than control T-cells in response to all four patient samples (Figure 4b). For 3/4 primary AML samples, IFN $\gamma$  secretion by HA-FR $\beta$  CAR T-cells was comparable to that achieved using THP1 cells, suggesting robust activity against patient tumor. The viability of cryopreserved patient samples was low, and standard lysis assays were not possible. We therefore evaluated CD107 expression on CAR<sup>+</sup> T-cells as a well-accepted surrogate for lytic function<sup>28</sup>. HA-FR $\beta$  CAR T-cells exhibited significantly higher CD107 expression

following 6h culture with primary AML (Figure 4c) than control T-cells, confirming the potential for clinical responses in AML patients using potent HA-FR $\beta$  CAR T-cells.

### High affinity FR $\beta$ IgG reveals increasing FR $\beta$ expression along myeloid differentiation in healthy hematopoietic cells

We next evaluated the potential for off-tumor recognition of FR $\beta$  in healthy tissues. Although previously reported<sup>29</sup>, we did not detect FR $\beta$  in HSCs using LA-FR $\beta$  IgG<sup>15</sup>. We hypothesized that its affinity may not permit sensitive detection of low levels of FR $\beta$  described elsewhere. Therefore, we used HA-FR $\beta$  IgG to investigate FR $\beta$  expression in CD34<sup>+</sup> BM HSCs from 5 healthy adults. In contrast to LA-FR $\beta$  IgG, we were able to detect very low surface FR $\beta$  in HSCs from most donors (Figure 5a). FR $\beta$  expression has been previously described in mature myeloid cells,<sup>30–32</sup> however, expression in BM progenitors has not been well characterized. Using myeloid markers (CD123, CD33, CD14), we found increasing FR $\beta$  expression during myeloid differentiation, with highest levels found in mature CD14<sup>+</sup> monocytes (Figure 5a). Other BM lineages were FR $\beta$ -negative (data not shown). In addition, we assayed peripheral blood (PB) for FR $\beta$  expression using HA-FR $\beta$  IgG. Consistent with previous results, we confirmed lack of expression in PB T-cells, B-cells, NK cells, and granulocytes (Figure 5b). PB FR $\beta$  expression was limited to CD14<sup>+</sup> monocytes, however, HA-FR $\beta$  IgG revealed ~70% (Mean 66.6%,  $\pm$  2.44% SEM) of PB monocytes express FR $\beta$ , whereas LA-FR $\beta$  IgG detection indicated <20% (Mean 15.2%,  $\pm$  3.24% SEM) (Figure 5c).

### High affinity FR $\beta$ CAR T-cells specifically eliminate FR $\beta$ <sup>+</sup> myeloid-lineage cells without toxicity against HSCs

To assess HSC toxicity, we conducted colony-forming (CFU) assays following co-culture with CAR T-cells. We did not observe inhibition of total or lineage-specific colony formation by HSCs under any condition (Figure 6a). These results suggest that very low FR $\beta$  expression observed in some CD34<sup>+</sup> donors was insufficient to activate FR $\beta$ -directed CAR T-cells. However, surface FR $\beta$  expression increases along BM myeloid differentiation and could activate HA-FR $\beta$  CAR T-cells. We co-cultured total CD34<sup>(-)</sup> BM cells with CAR T-cells and assessed the phenotype of surviving cells after 5h (Figure 6b). Extensive loss of viable myeloid-lineage (CD33<sup>+</sup>) target cells was not observed, however, HA-FR $\beta$  CAR T-cells clearly eliminated FR $\beta$ <sup>+</sup> CD33<sup>+</sup> myeloid cells (Figure 6b), suggesting that toxicity may be limited to the subset of FR $\beta$ <sup>+</sup> BM resident myeloid cells with neighboring FR $\beta$ <sup>(-)</sup> BM cells selectively spared. In accordance with their high FR $\beta$  expression, HA-FR $\beta$  CAR T-cells exhibited specific lysis of PB monocytes *in vitro* (Figure 6c).

To assess the impact of targeting FR $\beta$  in the native BM microenvironment, NSG mice reconstituted with human adult BM CD34<sup>+</sup> HSCs were treated with HA-FR $\beta$  or CD19 control CAR T cells derived from autologous BM T-cells (Figure S8a–b). Similar to *in vitro* experiments, BM HSCs or myeloid progenitor cells were not decreased after treatment with HA-FR $\beta$  CAR, however, CD19 control CAR T-cells decreased CD19<sup>+</sup> lymphoid-lineage BM cells (Figure S8d–g). Surprisingly, total CD14<sup>+</sup> monocytes were not significantly depleted by HA-FR $\beta$  CAR T-cells in this model (Figure S8c and h). However, we noted that FR $\beta$  expression in CD14<sup>+</sup> monocytes from these mice (13.9% FR $\beta$ <sup>+</sup>) was substantially lower



than that observed in fresh donor PB monocytes (70% FR $\beta^+$ ) (Figure S8i, Figure 5c). Despite this lower overall expression, HA-FR $\beta$  CAR T-cells still efficiently depleted FR $\beta^{\text{hi}}$  monocytes, resulting in decreased expression in monocytes from HA-FR $\beta$  CAR T-cell treated mice (mean 5.4% FR $\beta^+$ ) compared to CD19 control treated mice (mean 13.9% FR $\beta^+$ ) (Figure S7i). These data suggest that monocytes with the highest expression of FR $\beta$  expressed were depleted by HA-FR $\beta$  CAR T-cells *in vivo*.

### Transient high affinity FR $\beta$ mRNA CAR T-cells retain effective anti-tumor activity

Given that HA-FR $\beta$  CAR T-cells can eliminate both FR $\beta^+$  tumor and healthy myeloid cells but not HSCs, we reasoned that short-term CAR expression during T-cell therapy might allow for upfront tumor cell destruction, with eventual healthy myeloid cell repopulation from normal HSCs. Thus, we developed a transient HA-FR $\beta$  CAR model using mRNA electroporation of T-cells. One day post-electroporation, both HA-Z and HA-28Z CARs were highly expressed in T-cells with gradual decrease over time (Figure 7a), coinciding with a similar reduction in THP1 lysis (Figure 7b). mRNA and lentiviral HA-FR $\beta$  CAR T-cells displayed similar *in vitro* functional reactivity (Figure S9). We selected first generation HA-FR $\beta$  mRNA for *in vivo* T-cell evaluation as we reproducibly observed greater stability of HA-Z mRNA expression and never observed appreciable advantages using CD28 in lentiviral CARs. The activity of HA-Z lentiviral and mRNA CAR T-cells was assessed against disseminated THP1 delivered IV. Although not as robust as lentiviral CAR, HA-Z mRNA CAR T-cells significantly delayed disseminated THP1 tumor growth compared to CD19-Z mRNA T-cells (Figure 7c). These results suggest that mRNA delivery of the HA-FR $\beta$  CAR platform could be used transiently to eliminate FR $\beta^+$  tumor cells.

## Discussion

Utilizing a higher affinity scFv, we have greatly optimized our platform for robust targeting FR $\beta^+$  AML. HA-FR $\beta$  CAR T-cells reproducibly out-performed LA-FR $\beta$  CAR T-cells as demonstrated by significantly enhanced *in vitro* cytokine secretion, activation marker expression, cell lysis, and *in vivo* anti-leukemic activity.

HA-FR $\beta$  IgG allowed sensitive detection of very low levels of FR $\beta$  in hematopoietic cells not detectable by LA-FR $\beta$  IgG. Our results highlight the importance of antibody affinity when evaluating normal tissue expression for preclinical evaluation of new CAR targets. In addition, the field may find it useful to employ the scFv of the CAR for antibody-based analysis of tissue expression as this may best correlate with CAR recognition. Supporting this notion, we found that target cells not bound by LA-IgG (e.g. MV411 or BM progenitors) were not substantially targeted by LA-FR $\beta$  CAR T-cells.

The scFv affinity is considered critically important to CAR T-cell function, with a general consensus that higher affinity reduces the activation threshold, increasing T-cell activity at lower levels of antigen present. However, this aspect of CAR T-cell design is historically under-studied. Chmielewski *et al* developed CARs targeting hErbB2 with scFv affinities ranging from  $10^{-7}$  to  $10^{-11}$  nM, and established a threshold of  $10^{-8}$  below which CAR T-cells responded similarly to all levels of antigen, and above which CAR T-cells only responded to high levels of antigen<sup>16</sup>. Hudecek and colleagues observed increased anti-

tumor efficacy from ROR1-directed CAR T-cells with  $5.6 \times 10^{-10}$  nM  $K_D$  compared to  $6.5 \times 10^{-8}$  nM  $K_D$  scFvs<sup>17</sup>. We recently reported that FR $\alpha$  CAR T-cells bearing a high affinity scFv were more sensitive to low levels of FR $\alpha$  expression on healthy cells, increasing the risk for toxicity compared to intermediate affinity FR $\alpha$  CAR T-cells<sup>33</sup>. Our experience with FR $\beta$  CAR T-cells is in agreement with these findings. LA-FR $\beta$  CAR T-cells showed strong *in vitro* function only in response to high levels of antigen in C30-FR $\beta$  with reduced reactivity against lower-expressing AML lines THP1 and MV411. HA-FR $\beta$  CAR T-cells displayed strong reactivity against C30-FR $\beta$ , THP1, and MV411 without large differences in cytokine secretion in response to different levels of FR $\beta$ .

We hypothesize that the remarkable difference in LA-FR $\beta$  and HA-FR $\beta$  CAR T-cell function is related to affinity, however, it is formally possible that they recognize different epitopes of FR $\beta$ . For other CAR platforms, epitope proximity to the cell surface can drastically alter CAR performance<sup>34, 35</sup>. Our blocking studies showed that LA-FR $\beta$  and HA-FR $\beta$  IgGs inhibit the binding capability and/or CAR function of the other platform suggesting a nearby region is recognized. In addition, the two scFvs share identical heavy chain sequences with only 13 amino acid changes in the light chain, an overall 95% sequence homology. The highly similar sequences further suggest these two scFvs do not recognize dissimilar epitopes.

Generally, costimulatory domains provide functional improvement beyond first generation CAR platforms<sup>22, 36-39</sup>. Notably, both HA-Z and HA-28Z FR $\beta$  CAR T-cells were highly functional *in vitro* and resulted in complete tumor regression *in vivo*. To our knowledge, this is the first report of second generation CAR activity showing no improved *in vivo* benefit over first generation. We have observed varying levels of costimulatory ligands in AML cell lines<sup>15</sup>. Therefore, costimulation through natural receptors may compensate for the lack of costimulation in HA-Z CARs in the context of targeting AML. Costimulation through TNFR family members (4-1BB, CD27, or OX40) could further increase the persistence of HA-FR $\beta$  CAR T-cells beyond Z or 28Z, as reported elsewhere<sup>38, 40, 41</sup>. However, as discussed below, long-term persistence is likely not desirable for HA-FR $\beta$  CAR T-cells.

Encouragingly, even with highly potent HA-FR $\beta$  CARs, we did not see evidence of HSC destruction using *in vitro* CFU assays or *in vivo* humanized mouse models. This could be important as reports of gross BM toxicity have been described using CAR T-cells directed against AML antigens CD123 and CD33<sup>12, 14</sup>. Therefore, HA-FR $\beta$  CAR T-cells could potentially be applied with a reduced risk for BM HSC destruction compared to CD123 or CD33 CAR T-cells. However, FR $\beta$  expression does increase along myeloid-lineage differentiation with a distinctly later phase of expression in hematopoietic differentiation compared to CD123 and CD33. Accordingly, HA-FR $\beta$  CAR T-cells can lyse more mature myeloid lineage target cells. Therefore, FR $\beta$  CAR T-cell therapy may be well suited as an adjunct to be applied following myeloablation in advance of stem cell transplant, a common treatment modality for AML.

While ongoing depletion of healthy B-cells in patients treated with lentiviral CD19 CAR T-cells is managed through IgG replacement therapy, an analogous regimen to cope with lifelong myeloid depletion is not available. As such, long-term persistence of HA-FR $\beta$  CAR

T-cells is highly undesirable. Transient CAR expression in T-cells could allow for short-term tumor destruction while avoiding long-term myeloid loss. Multiple doses of HA-FR $\beta$  mRNA CAR T-cells significantly delayed THP1 growth *in vivo*. The HA-FR $\beta$  CAR sequence is fully human derived, decreasing the propensity for transgene immunogenicity which produced anaphylaxis after repeated administration of murine-derived CAR T-cells<sup>42</sup>. Alternatively, a suicide gene or inducible CAR approach could be used in combination with lentiviral HA-FR $\beta$  CAR T-cells to obtain complete tumor destruction before CAR depletion. In any case, transient treatment with HA-FR $\beta$  CAR T-cells appears to be a promising therapy for FR $\beta$ <sup>+</sup> AML while decreasing the risk for long-term myeloid toxicity.

## Supplementary Material

Refer to Web version on PubMed Central for supplementary material.

## Acknowledgments

This work was supported by grants from the NIH (RO1-CA168900; D.J.P.) and (T32-AI070099; R.C.L.) and by the Intramural Research Program of the Center for Cancer Research, National Cancer Institute, National Institutes of Health (D.S.D). We would like to acknowledge Gwenn Danet-Desnoyers, Tony Secreto, Josh Glover, and Winifred Trotman at the SCXC for their assistance with leukemia and BM acquisition and xenograft services. Bioluminescent imaging was supported by the University of Pennsylvania small animal imaging core facility.

## References

1. Howlader AMN, N.; Krapcho, M.; Garshell, J.; Miller, D.; Altekruse, SF.; Kosary, CL.; Yu, M.; Ruhl, J.; Tatalovich, Z.; Mariotto, A.; Lewis, DR.; Chen, HS.; Feuer, EJ.; Cronin, KA. National Cancer Institute; SEER Cancer Statistics Review (CSR) 1975–2012. [http://seer.cancer.gov/csr/1975\\_2012/](http://seer.cancer.gov/csr/1975_2012/) 1975–2012. p. based on November 2014 SEER data submission, posted to the SEER web site, April 2015
2. Robak T, Wierzbowska A. Current and emerging therapies for acute myeloid leukemia. *Clin Ther*. 2009; 31(Pt 2):2349–2370. [PubMed: 20110045]
3. Kanate AS, Pasquini MC, Hari PN, Hamadani M. Allogeneic hematopoietic cell transplant for acute myeloid leukemia: Current state in 2013 and future directions. *World J Stem Cells*. 2014 Apr 26; 6(2):69–81. [PubMed: 24772235]
4. Jacobsohn DA, Vogelsang GB. Acute graft versus host disease. *Orphanet J Rare Dis*. 2007; 2:35. [PubMed: 17784964]
5. Hahn T, McCarthy PL Jr, Zhang MJ, Wang D, Arora M, Frangoul H, et al. Risk factors for acute graft-versus-host disease after human leukocyte antigen-identical sibling transplants for adults with leukemia. *J Clin Oncol*. 2008 Dec 10; 26(35):5728–5734. [PubMed: 18981462]
6. Grupp SA, Kalos M, Barrett D, Aplenc R, Porter DL, Rheingold SR, et al. Chimeric antigen receptor-modified T cells for acute lymphoid leukemia. *N Engl J Med*. 2013 Apr 18; 368(16):1509–1518. [PubMed: 23527958]
7. Brentjens RJ, Davila ML, Riviere I, Park J, Wang X, Cowell LG, et al. CD19-targeted T cells rapidly induce molecular remissions in adults with chemotherapy-refractory acute lymphoblastic leukemia. *Sci Transl Med*. 2013 Mar 20.5(177):177ra138.
8. Lee DW, Kochenderfer JN, Stetler-Stevenson M, Cui YK, Delbrook C, Feldman SA, et al. T cells expressing CD19 chimeric antigen receptors for acute lymphoblastic leukaemia in children and young adults: a phase 1 dose-escalation trial. *Lancet*. 2015 Feb 7; 385(9967):517–528. [PubMed: 25319501]
9. Gross G, Waks T, Eshhar Z. Expression of immunoglobulin-T-cell receptor chimeric molecules as functional receptors with antibody-type specificity. *Proc Natl Acad Sci U S A*. 1989 Dec; 86(24):10024–10028. [PubMed: 2513569]

10. Tettamanti S, Marin V, Pizzitola I, Magnani CF, Giordano Attianese GM, Cribioli E, et al. Targeting of acute myeloid leukaemia by cytokine-induced killer cells redirected with a novel CD123-specific chimeric antigen receptor. *Br J Haematol*. 2013 May; 161(3):389–401. [PubMed: 23432359]
11. Mardiros A, Dos Santos C, McDonald T, Brown CE, Wang X, Budde LE, et al. T cells expressing CD123-specific chimeric antigen receptors exhibit specific cytolytic effector functions and antitumor effects against human acute myeloid leukemia. *Blood*. 2013 Oct 31; 122(18):3138–3148. [PubMed: 24030378]
12. Gill S, Tasian SK, Ruella M, Shestova O, Li Y, Porter DL, et al. Preclinical targeting of human acute myeloid leukemia and myeloablation using chimeric antigen receptor-modified T cells. *Blood*. 2014 Apr 10; 123(15):2343–2354. [PubMed: 24596416]
13. Dutour A, Marin V, Pizzitola I, Valsesia-Wittmann S, Lee D, Yvon E, et al. In Vitro and In Vivo Antitumor Effect of Anti-CD33 Chimeric Receptor-Expressing EBV-CTL against CD33 Acute Myeloid Leukemia. *Adv Hematol*. 2012; 2012:683065. [PubMed: 22272203]
14. Kenderian SS, Ruella M, Shestova O, Klichinsky M, Aikawa V, Morrissette JJ, et al. CD33 Specific Chimeric Antigen Receptor T Cells Exhibit Potent Preclinical Activity against Human Acute Myeloid Leukemia. *Leukemia*. 2015 Feb 27.
15. Lynn RC, Poussin M, Kalota A, Feng Y, Low PS, Dimitrov DS, et al. Targeting of folate receptor-beta on acute myeloid leukemia blasts with chimeric antigen receptor expressing T cells. *Blood*. 2015 Apr 17.
16. Chmielewski M, Hombach A, Heuser C, Adams GP, Abken H. T cell activation by antibody-like immunoreceptors: increase in affinity of the single-chain fragment domain above threshold does not increase T cell activation against antigen-positive target cells but decreases selectivity. *J Immunol*. 2004 Dec 15; 173(12):7647–7653. [PubMed: 15585893]
17. Hudecek M, Lupo-Stanghellini MT, Kosasih PL, Sommermeyer D, Jensen MC, Rader C, et al. Receptor affinity and extracellular domain modifications affect tumor recognition by ROR1-specific chimeric antigen receptor T cells. *Clin Cancer Res*. 2013 Jun 15; 19(12):3153–3164. [PubMed: 23620405]
18. Morgan RA, Yang JC, Kitano M, Dudley ME, Laurencot CM, Rosenberg SA. Case report of a serious adverse event following the administration of T cells transduced with a chimeric antigen receptor recognizing ERBB2. *Mol Ther*. 2010 Apr; 18(4):843–851. [PubMed: 20179677]
19. Lamers CH, Sleijfer S, Vulto AG, Kruit WH, Kliffen M, Debets R, et al. Treatment of metastatic renal cell carcinoma with autologous T-lymphocytes genetically retargeted against carbonic anhydrase IX: first clinical experience. *J Clin Oncol*. 2006 May 1; 24(13):e20–e22. [PubMed: 16648493]
20. Hinrichs CS, Restifo NP. Reassessing target antigens for adoptive T-cell therapy. *Nat Biotechnol*. 2013 Nov; 31(11):999–1008. [PubMed: 24142051]
21. Feng Y, Zhu Z, Xiao X, Choudhry V, Barrett JC, Dimitrov DS. Novel human monoclonal antibodies to insulin-like growth factor (IGF)-II that potently inhibit the IGF receptor type I signal transduction function. *Mol Cancer Ther*. 2006 Jan; 5(1):114–120. [PubMed: 16432169]
22. Lanitis E, Poussin M, Hagemann IS, Coukos G, Sandaltzopoulos R, Scholler N, et al. Redirected antitumor activity of primary human lymphocytes transduced with a fully human anti-mesothelin chimeric receptor. *Mol Ther*. 2012 Mar; 20(3):633–643. [PubMed: 22127019]
23. Godwin AK, Meister A, O'Dwyer PJ, Huang CS, Hamilton TC, Anderson ME. High resistance to cisplatin in human ovarian cancer cell lines is associated with marked increase of glutathione synthesis. *Proc Natl Acad Sci U S A*. 1992 Apr 1; 89(7):3070–3074. [PubMed: 1348364]
24. Schutsky K, Song DG, Lynn R, Smith JB, Poussin M, Figini M, et al. Rigorous optimization and validation of potent RNA CAR T cell therapy for the treatment of common epithelial cancers expressing folate receptor. *Oncotarget*. 2015 Sep 2.
25. Feng Y, Shen J, Streaker ED, Lockwood M, Zhu Z, Low PS, et al. A folate receptor beta-specific human monoclonal antibody recognizes activated macrophage of rheumatoid patients and mediates antibody-dependent cell-mediated cytotoxicity. *Arthritis Res Ther*. 2011; 13(2):R59. [PubMed: 21477314]

26. Ross JF, Wang H, Behm FG, Mathew P, Wu M, Booth R, et al. Folate receptor type beta is a neutrophilic lineage marker and is differentially expressed in myeloid leukemia. *Cancer*. 1999 Jan 15; 85(2):348–357. [PubMed: 10023702]
27. Pan XQ. Strategy for the treatment of acute myelogenous leukemia based on folate receptor beta - targeted liposomal doxorubicin combined with receptor induction using all-trans retinoic acid. *Blood*. 2002; 100(2):594–602. [PubMed: 12091353]
28. Betts MR, Brenchley JM, Price DA, De Rosa SC, Douek DC, Roederer M, et al. Sensitive and viable identification of antigen-specific CD8+ T cells by a flow cytometric assay for degranulation. *J Immunol Methods*. 2003 Oct 1; 281(1–2):65–78. [PubMed: 14580882]
29. Reddy JA, Haneline LS, Srour EF, Antony AC, Clapp DW, Low PS. Expression and functional characterization of the beta-isoform of the folate receptor on CD34(+) cells. *Blood*. 1999 Jun 1; 93(11):3940–3948. [PubMed: 10339503]
30. Shen F, Ross JF, Wang X, Ratnam M. Identification of a novel folate receptor, a truncated receptor, and receptor type beta in hematopoietic cells: cDNA cloning, expression, immunoreactivity, and tissue specificity. *Biochemistry*. 1994 Feb 8; 33(5):1209–1215. [PubMed: 8110752]
31. Nakashima-Matsushita N, Homma T, Yu S, Matsuda T, Sunahara N, Nakamura T, et al. Selective expression of folate receptor beta and its possible role in methotrexate transport in synovial macrophages from patients with rheumatoid arthritis. *Arthritis Rheum*. 1999 Aug; 42(8):1609–1616. [PubMed: 10446858]
32. Shen J, Hilgenbrink AR, Xia W, Feng Y, Dimitrov DS, Lockwood MB, et al. Folate receptor-beta constitutes a marker for human proinflammatory monocytes. *J Leukoc Biol*. 2014 Oct; 96(4):563–570. [PubMed: 25015955]
33. Song DG, Ye Q, Poussin M, Liu L, Figini M, Powell DJ Jr. A fully human chimeric antigen receptor with potent activity against cancer cells but reduced risk for off-tumor toxicity. *Oncotarget*. 2015 Jun 19.
34. Hombach AA, Schildgen V, Heuser C, Finnern R, Gilham DE, Abken H. T cell activation by antibody-like immunoreceptors: the position of the binding epitope within the target molecule determines the efficiency of activation of redirected T cells. *J Immunol*. 2007 Apr 1; 178(7):4650–4657. [PubMed: 17372024]
35. James SE, Greenberg PD, Jensen MC, Lin Y, Wang J, Till BG, et al. Antigen sensitivity of CD22-specific chimeric TCR is modulated by target epitope distance from the cell membrane. *J Immunol*. 2008 May 15; 180(10):7028–7038. [PubMed: 18453625]
36. Kowolik CM, Topp MS, Gonzalez S, Pfeiffer T, Olivares S, Gonzalez N, et al. CD28 costimulation provided through a CD19-specific chimeric antigen receptor enhances in vivo persistence and antitumor efficacy of adoptively transferred T cells. *Cancer Res*. 2006 Nov 15; 66(22):10995–11004. [PubMed: 17108138]
37. Savoldo B, Ramos CA, Liu E, Mims MP, Keating MJ, Carrum G, et al. CD28 costimulation improves expansion and persistence of chimeric antigen receptor-modified T cells in lymphoma patients. *J Clin Invest*. 2011 May; 121(5):1822–1826. [PubMed: 21540550]
38. Carpenito C, Milone MC, Hassan R, Simonet JC, Lakhai M, Suhoski MM, et al. Control of large, established tumor xenografts with genetically retargeted human T cells containing CD28 and CD137 domains. *Proc Natl Acad Sci U S A*. 2009 Mar 3; 106(9):3360–3365. [PubMed: 19211796]
39. Song DG, Ye Q, Carpenito C, Poussin M, Wang LP, Ji C, et al. In vivo persistence, tumor localization, and antitumor activity of CAR-engineered T cells is enhanced by costimulatory signaling through CD137 (4-1BB). *Cancer Res*. 2011 Jul 1; 71(13):4617–4627. [PubMed: 21546571]
40. Milone MC, Fish JD, Carpenito C, Carroll RG, Binder GK, Teachey D, et al. Chimeric receptors containing CD137 signal transduction domains mediate enhanced survival of T cells and increased antileukemic efficacy in vivo. *Mol Ther*. 2009 Aug; 17(8):1453–1464. [PubMed: 19384291]
41. Song DG, Ye Q, Poussin M, Harms GM, Figini M, Powell DJ Jr. CD27 costimulation augments the survival and antitumor activity of redirected human T cells in vivo. *Blood*. 2012 Jan 19; 119(3):696–706. [PubMed: 22117050]

42. Maus MV, Haas AR, Beatty GL, Albelda SM, Levine BL, Liu X, et al. T cells expressing chimeric antigen receptors can cause anaphylaxis in humans. *Cancer Immunol Res.* 2013 Jul; 1(1):26–31.

Author Manuscript

Author Manuscript

Author Manuscript

Author Manuscript

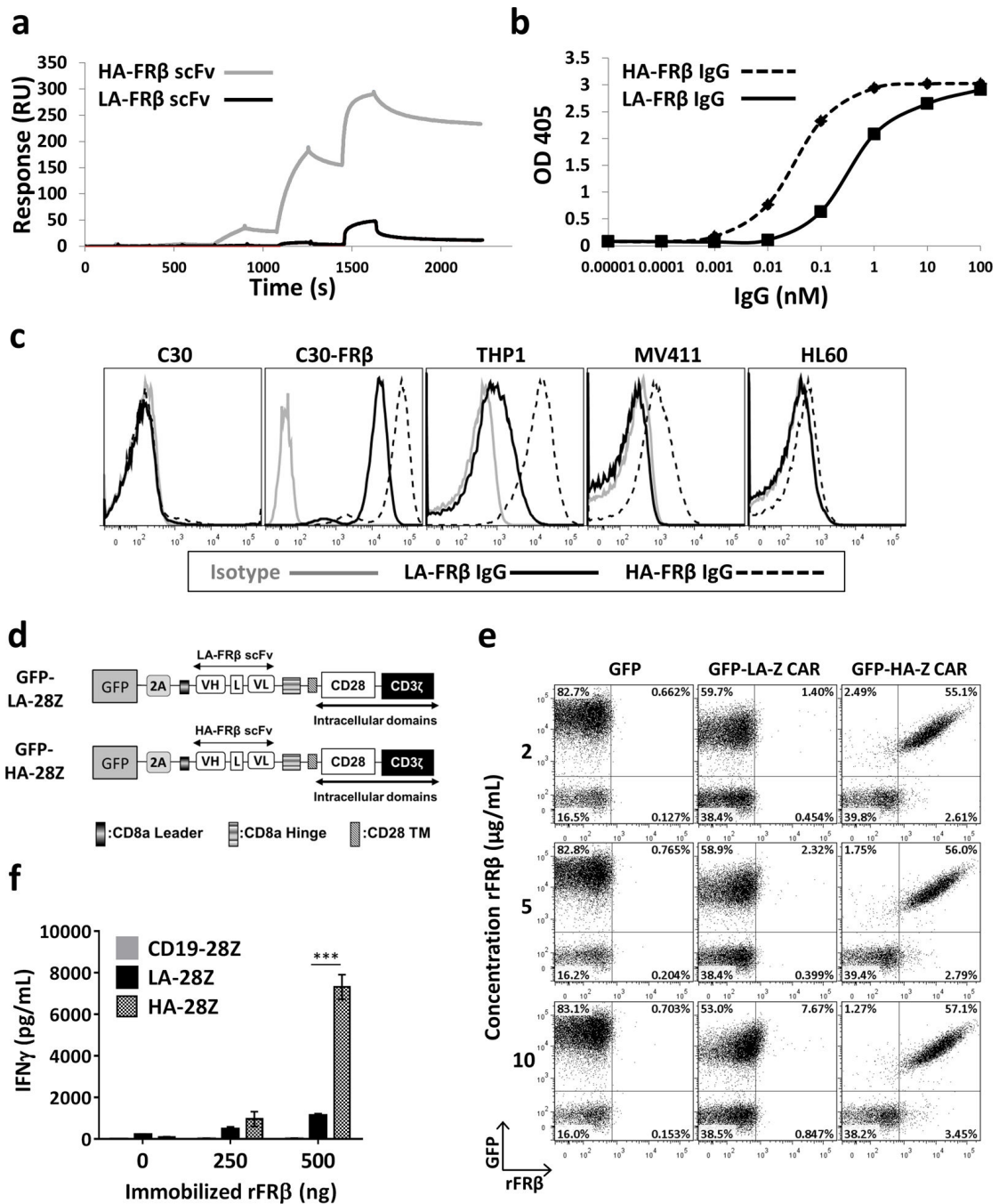


**Figure 1. Isolation and characterization of a higher affinity FR $\beta$  scFv**

(a) Increasing concentrations (0.04, 0.4, 4, 40, and 400 nM) of soluble scFvs were applied to human FR $\beta$ -coated chips and affinity was measured by plasmon resonance with Biacore $\times$ 100. Binding of LA-FR $\beta$  and HA-FR $\beta$  IgG to (b) immobilized rFR $\beta$  measured by ELISA or (c) cell-surface FR $\beta$  measured by flow cytometry in the indicated cell lines. (d) Representative schematics of lentiviral CAR constructs (full list in Figure S4a). (e) Binding of LA-FR $\beta$  and HA-FR $\beta$  CAR $^{+}$  (GFP $^{+}$ ) T cells to soluble rFR $\beta$ . (f) IFN $\gamma$  secretion following 24h culture of LA-FR $\beta$  and HA-FR $\beta$  CAR T cells in rFR $\beta$ -coated plates. CD19-28Z CAR T

cells were used as a negative control. Error bars represent mean  $\pm$  SD of triplicate wells. scFv – single chain variable fragment, VH – variable heavy chain, L – linker, VL – variable light chain, TM – transmembrane domain, LA – low affinity FR $\beta$ , and HA – high affinity FR $\beta$ . (\* P < .05, \*\* P < .01, \*\*\* P < .001)

Author Manuscript

Author Manuscript

Author Manuscript

Author Manuscript



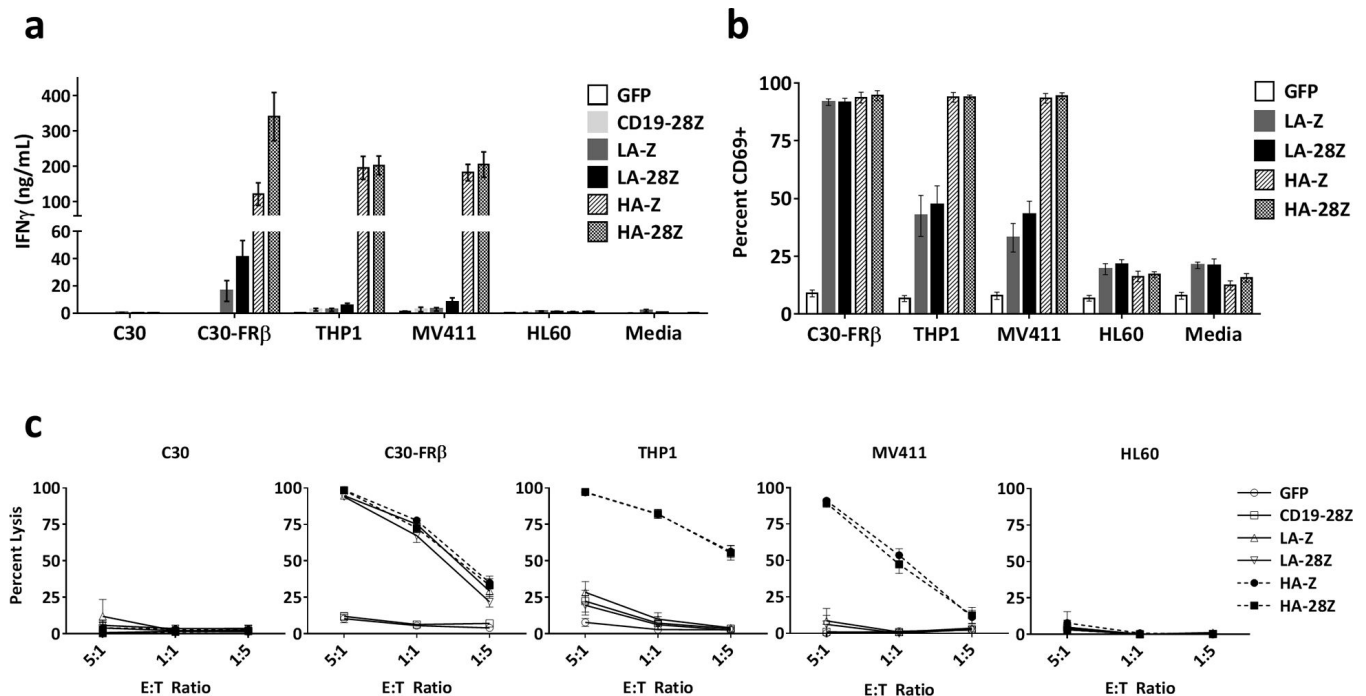


**Figure 2. High affinity FR $\beta$  CAR T cells demonstrate greater *in vitro* reactivity against FR $\beta$ <sup>+</sup> cell lines compared to low affinity FR $\beta$  CAR T cells**

**(a)** IFN $\gamma$  secretion following overnight co-culture of LA-FR $\beta$ , HA-FR $\beta$ , or control CAR T cells with the indicated cell lines. Error bars represent mean  $\pm$  SEM of n = 5 independent experiments each performed in triplicate. **(b)** CD69 expression on CAR T cells following overnight co-culture with the indicated target cells. Live, CD3<sup>+</sup> CAR<sup>+</sup> flow cytometry gates were used to assess percent CD69<sup>+</sup> CAR T cells. Error bars represent mean  $\pm$  SEM of n=4 independent experiments each performed in triplicate. (Note: unstimulated CAR<sup>+</sup> T-cells have ~20% CD69<sup>+</sup> cells at baseline as revealed in the Media control). **(c)** High lytic activity from HA-FR $\beta$  CAR T cells against FR $\beta$ <sup>+</sup> cell lines compared to LA-FR $\beta$  T cells and fLuc<sup>+</sup> target cells were co-cultured at the indicated E:T ratios. Percent lysis was assessed by residual target cell luminescence following overnight culture. Error bars represent mean  $\pm$  SEM of n = 5 independent experiments each performed in triplicate. Media indicates T cells cultured without target cells. GFP and/or CD19-28Z CAR T cells were used as controls. SEM – standard error, fLuc – firefly luciferase, LA – low affinity FR $\beta$ , HA – high affinity FR $\beta$ .

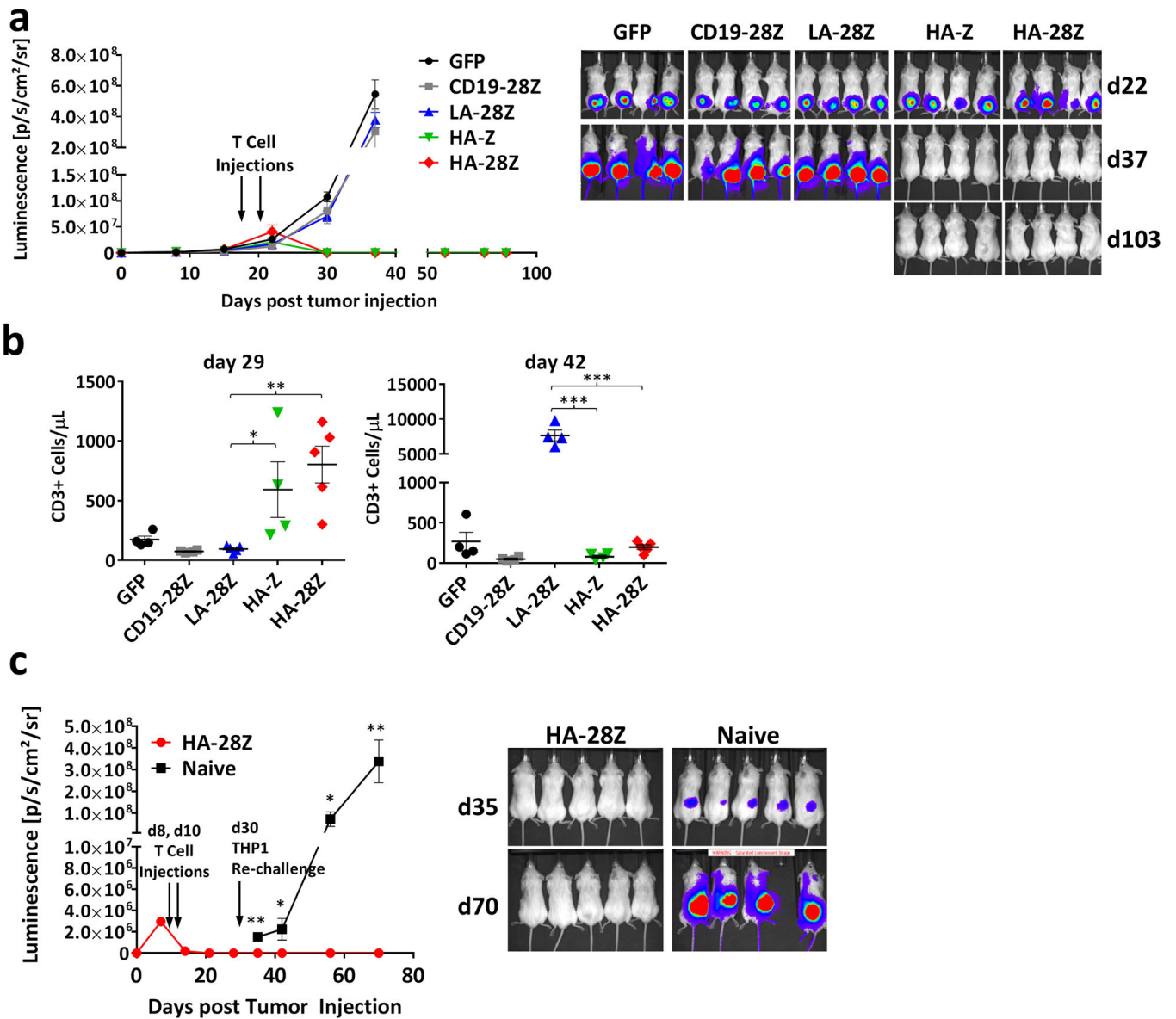


**Figure 3. High affinity FR $\beta$  CAR T cells display exceptional anti-leukemic activity *in vivo***  
 In panels a–b,  $5 \times 10^6$  fLuc-THP1 AML cells were injected sc into flanks of NSG mice.  $5 \times 10^6$  CAR<sup>+</sup> (or GFP<sup>+</sup>) T cells were injected IP on days 19 and 22 post tumor inoculation. **(a)** Tumor growth was monitored by tumor bioluminescence. **(b)** Peripheral blood T cell quantification on days 29 and 42 post tumor inoculation. Error bars represent mean  $\pm$  SEM of n=4–5 mice per group. In panel c, mice were injected with  $5 \times 10^6$  HA-28Z CAR T cells on days 8 and 10 following tumor inoculation. Following tumor clearance on day 30, HA-28Z treated mice were re-challenged and previously untreated (naïve) mice were challenged with  $5 \times 10^6$  fLuc-THP1. Tumor growth was monitored by bioluminescence **(c)**. Error bars represent mean  $\pm$  SEM of n=5 mice per group. fLuc – firefly luciferase, NSG – Nod/SCID/ $\gamma$ chain<sup>-/-</sup>, sc– subcutaneous, IP – intraperitoneal, SEM – standard error, LA – low affinity FR $\beta$ , HA – high affinity FR $\beta$ . (\* P < .05, \*\* P < .01, \*\*\* P < .001)

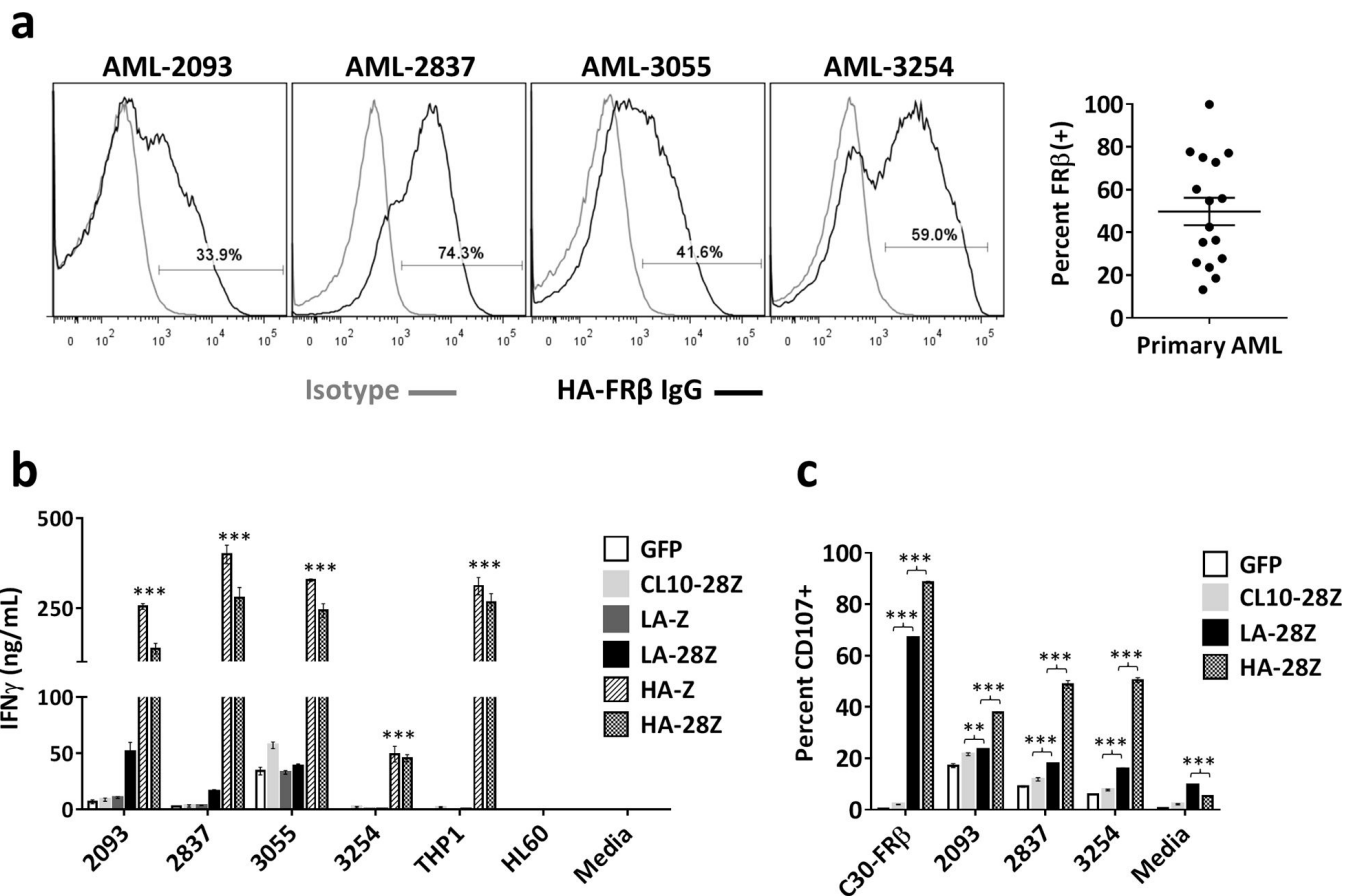


**Figure 4. High affinity FR $\beta$  CAR T cells are reactive against primary human AML**  
**(a)** FR $\beta$  expression in primary human peripheral blood cells isolated from AML patients. Live, CD33 $^{+}$  gates were used to assess FR $\beta$  expression by flow cytometry. (Gray histogram – isotype, black histogram – HA-FR $\beta$  IgG). 4 representative histograms shown. Percent FR $\beta^{+}$  blasts for n=16 patients is summarized to the right (Mean=49.8%). **(b)** IFN $\gamma$  secretion after overnight co-culture of indicated primary AML samples with CAR T cells. The CD19 CAR control was replaced with a murine FR $\beta$ -specific CL10-28Z CAR T-cell control because of the presence of CD19 $^{+}$  B cells in the patient blood samples. Error bars represent mean  $\pm$  SD of triplicate wells. One representative of 3 independent experiments shown. (\*\*\*) P < .001 for both HA-Z and HA-28Z compared to CL10-28Z control CAR T cells) **(c)** CD107 upregulation on CAR $^{+}$  T cells following 6h co-culture with primary AML patient cells. Live, CD3 $^{+}$ , CAR $^{+}$  gates were used to assess percent CD107 $^{+}$ . Error bars represent mean  $\pm$  SD of triplicate wells. One representative of 2 independent experiments shown. SD – standard deviation, LA – low affinity FR $\beta$ , HA – high affinity FR $\beta$ . (\*\* P < .01, \*\*\* P < .001)

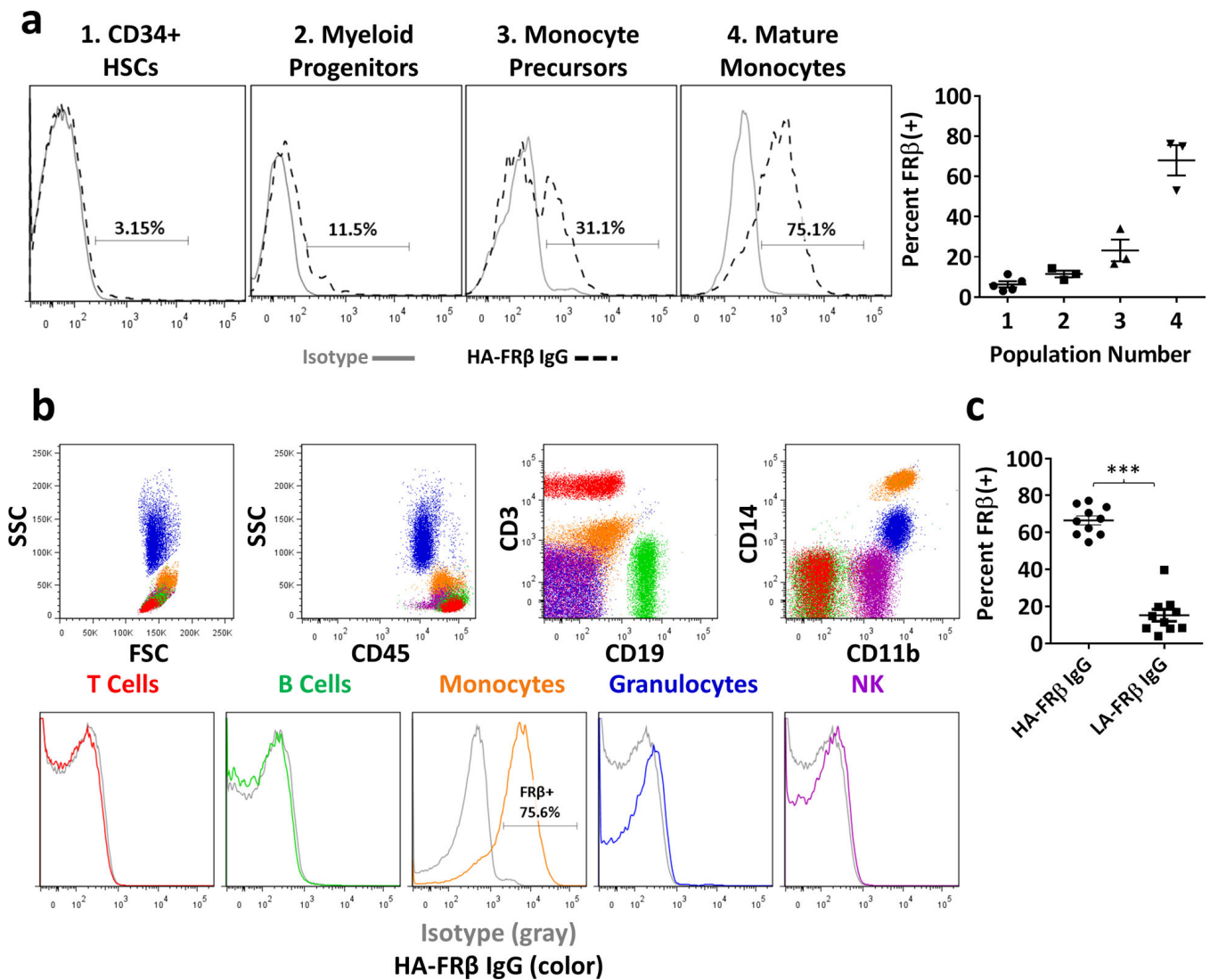


**Figure 5. High affinity FRβ IgG reveals increasing expression of FRβ along myeloid differentiation in healthy hematopoietic cells**

(a) FRβ expression in healthy adult BM. Representative histograms from one donor shown. Data from 3–5 independent donors is displayed to the right for the following populations: (1) CD34<sup>+</sup> HSCs (Mean 6.3% FRβ<sup>+</sup>, n=5). (2) Myeloid progenitors—CD123<sup>HI</sup>CD33<sup>(-)</sup>CD14<sup>(-)</sup> (Mean 11.4% FRβ<sup>+</sup>, n=3), (3) Monocyte precursors—CD123<sup>low</sup>, CD33<sup>+</sup>, CD14<sup>low</sup> (Mean 23.2% FRβ<sup>+</sup>, n=3), and (4) Mature monocytes—CD123<sup>(-)</sup>, CD33<sup>+</sup>, CD14<sup>HI</sup> (Mean 68.0% FRβ<sup>+</sup>, n=3). (Gray histogram— isotype, black dashed histogram – HA-FRβ IgG). (b) FRβ expression in peripheral blood cells. Upper panels – gating strategy to identify subsets. Lower panels – FRβ expression in indicated subsets. (Gray histogram— isotype, color histograms – HA-FRβ IgG) Red – T cells, Green – B cells, Orange – monocytes, Blue – granulocytes, Purple – NK cells. One representative of 3 independent donors shown. (c) Percent FRβ expression detected in peripheral blood monocytes (n=10) using HA-FRβ IgG (mean=66.6%) or LA-FRβ IgG (mean=15.2%) for flow cytometry. Error bars represent

mean  $\pm$  SEM. BM – bone marrow, HSCs – hematopoietic stem cells, SSC – side scatter, FSC – forward scatter, LA – low affinity FR $\beta$ , HA – high affinity FR $\beta$ . (\*\*\*) P < .001

Author Manuscript

Author Manuscript

Author Manuscript

Author Manuscript

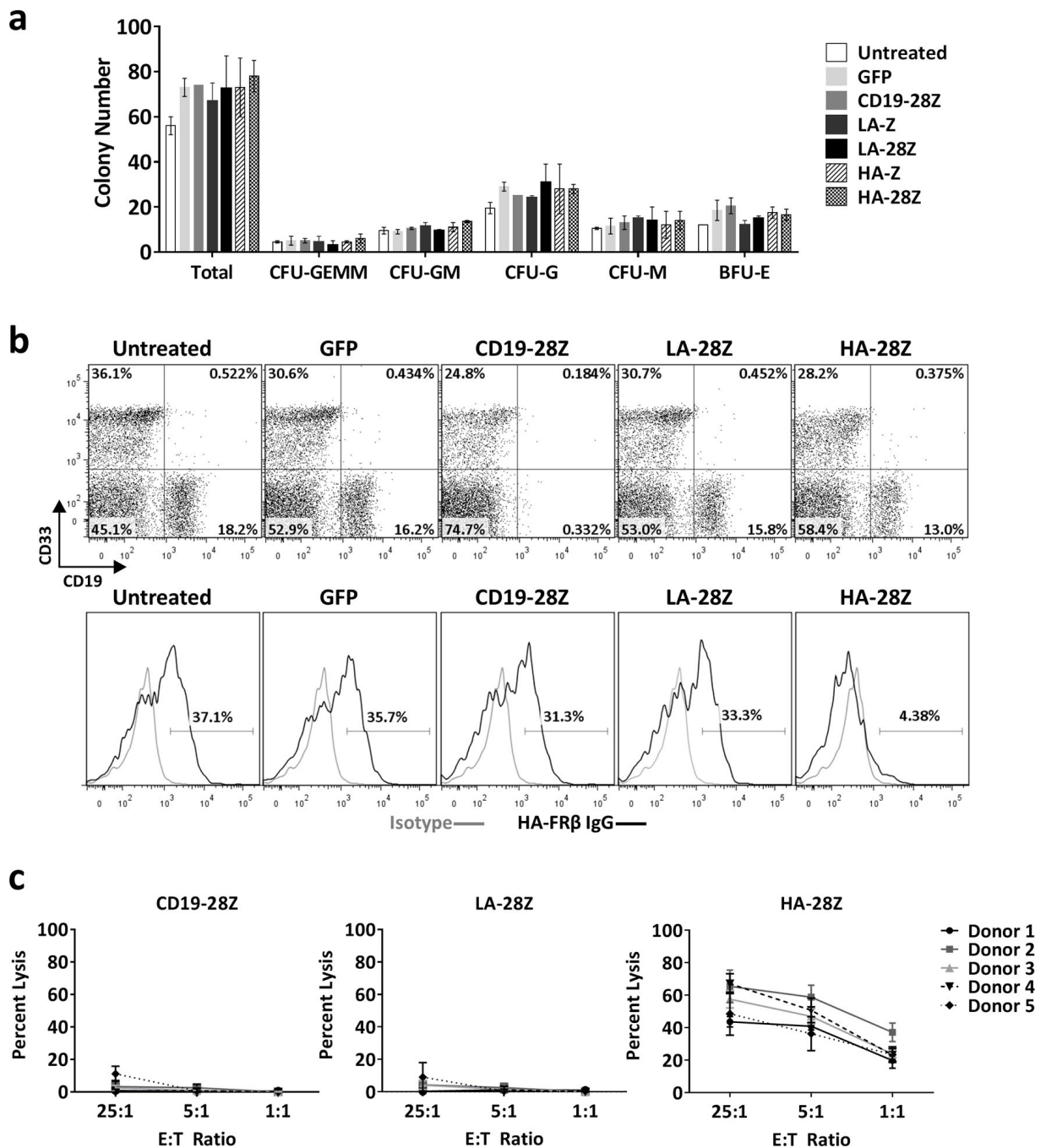
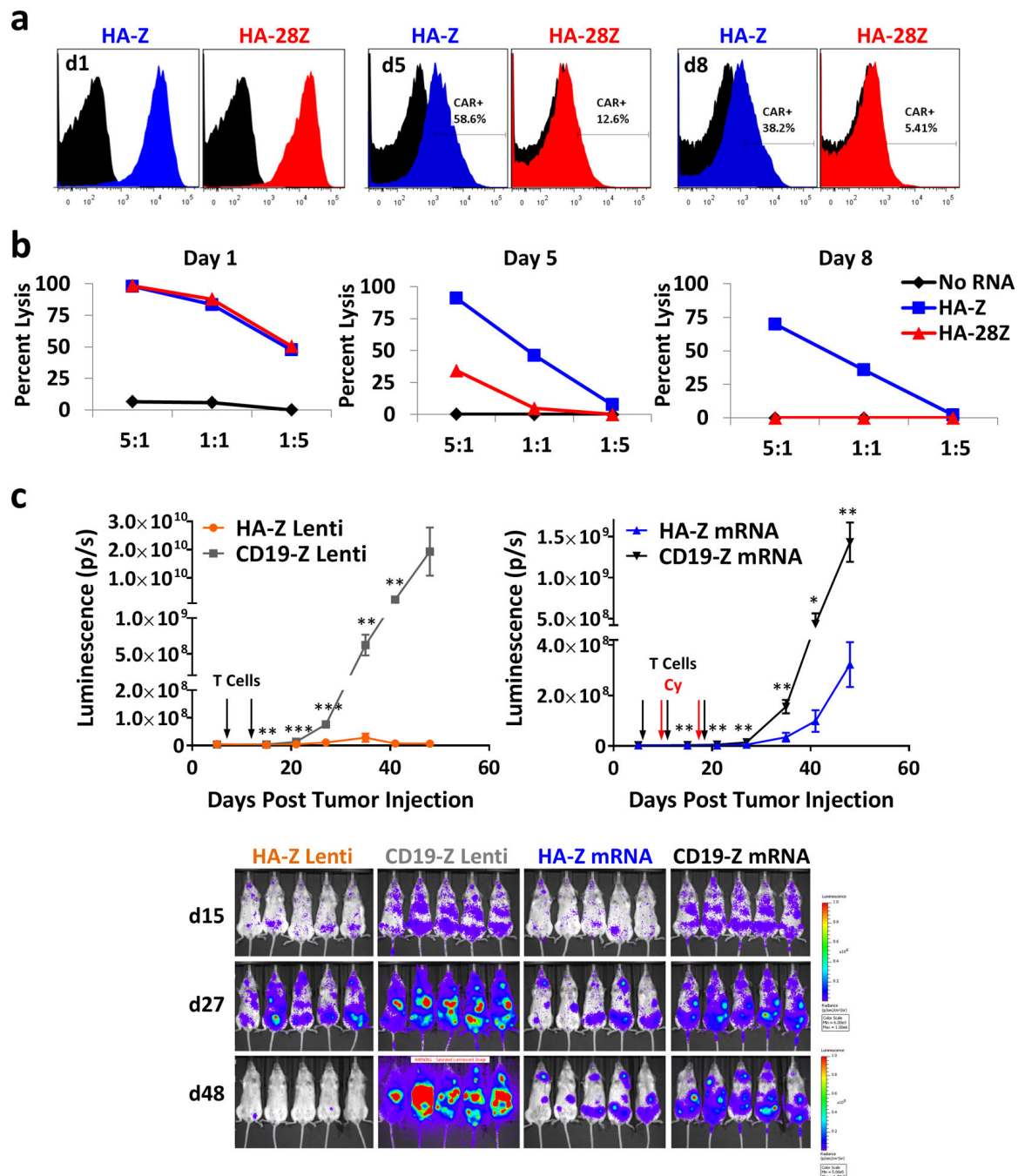


**Figure 6. High Affinity FR $\beta$  CAR T-cells specifically eliminate FR $\beta$ <sup>+</sup> myeloid lineage cells without toxicity against HSCs**

(a) Number of total and lineage specific colonies from CFU assay following 4h co-culture of 2000 CD34<sup>+</sup> and 2000 CAR<sup>+</sup> T cells. Error bars represent mean  $\pm$  SD of duplicate wells. One representative of 4 independent experiments is shown. (b) Phenotype of CD34<sup>(-)</sup> adult BM following 5h co-culture with CAR T cells. Untreated samples were cultured in the absence of T cells. Upper panels - frequency of CD33 and CD19 expression in total live, CD3<sup>(-)</sup> target cells surviving co-culture with the indicated T cells. Lower panels - FR $\beta$

Percent Lysis

expression in total live, CD3<sup>(-)</sup>CD33<sup>+</sup> myeloid lineage BM target cells surviving co-culture with the indicated T cells. (Gray histogram– isotype, black histogram – HA-FRβ IgG). One representative of 3 independent experiments is shown. (c) Percent lysis of isolated CD14<sup>+</sup> peripheral blood monocytes following 4h co-culture with CAR T cells at 25:1, 5:1, or 1:1 E:T ratios. Error bars represent mean ± SD of 6 replicate wells. 5 independent healthy monocyte donors were assessed. CFU– colony forming unit, GEMM–granulocyte/erythrocyte/monocyte/megakaryocyte, GM–granulocyte/monocyte, G–granulocyte, M–monocyte, BFU-E– erythroid blast forming unit, BM– bone marrow, SD– standard deviation, SEM– standard error, LA – low affinity FRβ, HA – high affinity FRβ.





CD19-Z Lenti CAR T cells on days 6 and 11, or  $10 \times 10^6$  HA-Z or CD19-Z mRNA CAR T cells on days 6, 11, and 18 post tumor injection via IV delivery. mRNA CAR T cells were injected 18h post-electroporation. Mice receiving mRNA CAR T cells also received 60mg/kg Cyclophosphamide (Cy) IP between T cell doses (days 10 and 17) to eliminate CAR-negative T cells between doses. Error bars represent mean  $\pm$  SEM of n=5 mice per group. IV– intravenous, IP– intraperitoneal, SEM– standard error, HA – high affinity FR $\beta$ . (\* P < .05, \*\* P < .01, \*\*\* P < .001)